2012 IEEE International Conference on Power Electronics, Drives and Energy Systems
December16-19, 2012, Bengaluru, India

Control of the Modular Multilevel Converter for Variable-speed Drives

Jae-Jung Jung, Hak-Jun Lee, and Seung-Ki Sul
Department of Electrical and Computer Engineering,
Seoul National University
1 Gwanak-ro, Gwanak-gu, Seoul 151-744, Republic of Korea
jjjzzz@eepel.snu.ac.kr

***Abstract*—This paper presents a control strategy of the entire frequency range operation for Modular Multilevel Converter (MMC), especially focusing on variable speed drive of an AC machine. The structure of MMC essentially requires energy balancing control so as to mitigate the voltage pulsation of each cell capacitor in converter arms. In the proposed control strategy, two operation modes are employed. One is a low frequency operation mode for start-up and low speed operation of the AC machine, and the other is a normal frequency operation mode from medium to rated speed of the AC machine. To reduce the pulsation, this paper proposes the energy balancing control strategies at each operation mode. Theoretically, the energy balancing control of the capacitors is prone to be unstable at low frequency operation. In order to prevent the instability, a special control strategy is introduced. The strategy exploits a common mode voltage and a circulating current with high frequency component in low frequency operation mode. With the proposed control scheme, the speed control range of the AC machine driven by MMC can be down to zero speed without instability of voltage of the cell capacitors. Experimental results for the energy balancing control are shown to demonstrate the effectiveness of the proposed control strategy.**

Keywords—modular multilevel converter, circulating currents, power balancing control, variable speed drives

I. INTRODUCTION

A Modular Multilevel Converter (MMC) is regarded as one of promising topologies in high power conversion system without bulky reactive components such as line-transformer, harmonic filter, and DC link reactor [1]-[3]. Compared to conventional voltage source converters, the MMC has modular structure which is made up of identical converter cells. Therefore, it has advantages such as easy adaptation to higher voltage level, easy maintenance and assembly, and fault tolerance. Due to these merits of the MMC, the researches applying MMC to HVDC system have been widely carried out and MMC has been used for high voltage DC transmission system [4]-[5]. Theoretically, the voltage pulsation of the capacitor of each cell is proportional to output phase current and inversely proportional to operating frequency [6]. So, it is inherently difficult to drive AC machine by MMC, that requires a starting torque and low speed steady state operation. In the recent studies [6]-[9], however, several control schemes of MMC have been introduced for variable speed AC motor drive application. They have presented principles for MMC operation over complete frequency range. But these studies do not precisely address the actual control strategies such as changing output frequency including standstill operation.

This paper proposes a control strategy to suppress the voltage fluctuation of the capacitor of each cell exploiting inner circulating current and high frequency component common mode voltage. Additionally, a switchover tactic between low frequency operation mode and normal frequency operation mode is described to drive AC machine in overall speed region. The proposed control scheme is based on energy balance between each cell capacitor and between upper and lower arm. The effectiveness of the proposed control strategy has been evaluated by experimental results.

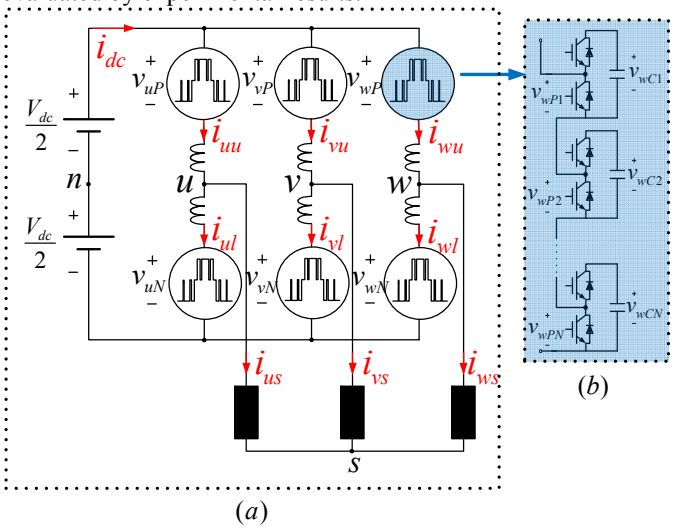

Figure 1. Circuit configuration of the MMC.

II. CONFIGURATION OF THE MMC AND PROPOSED CONTROL SCHEME

A. Configuration of the MMC

Fig. 1(a) shows the circuit configuration of the MMC. The MMC is composed of six arms, six arm inductors, and a DC-link voltage source. Each arm has cascaded N-identical cells, and each cell consists of one DC capacitor and two active switching devices. The cell modules are depicted in Fig. 1(b) in

978-1-4673-4508-8/12/$31.00 ©2012 IEEE

detail. In Fig. 1(a), first, i_{xu} and i_{xl} are the upper and lower arm currents, respectively, and i_{xs} is the output phase current, where the notation ' x ' represents u, v or w phase. The output phase current (i_{xs}) and circulating current (i_{xo}) are calculated from the upper and lower arm currents as described in (1)-(2). Therefore, the arm currents can be deduced as (3)-(4).

$$i_{xs} = i_{xu} - i_{xl} . \tag{1}$$

$$i_{xo} = \frac{i_{xu} + i_{xl}}{2} . \tag{2}$$

$$i_{xu} = \frac{1}{2} i_{xs} + i_{xo} . \tag{3}$$

$$i_{xl} = -\frac{1}{2} i_{xs} + i_{xo} . \tag{4}$$

The voltage relationship along x -phase loop can be expressed as (5)-(6) using KVL. Here, V_{dc} is DC-link voltage, v_{xP} and v_{xN} are the upper and lower arm voltages, respectively. v_{xn} is the pole voltage, and v_{xuL} and v_{xlL} stand for the voltage drop of each arm inductor in the upper and lower arm, respectively.

$$-\frac{V_{dc}}{2} + v_{xuL} + v_{xP} + v_{xn} = 0 . \tag{5}$$

$$\frac{V_{dc}}{2} - v_{xlL} - v_{xN} + v_{xn} = 0 . \tag{6}$$

First, (7) can be derived by subtracting (6) from (5), and (7) can be rewritten as (8) under the definition of $v_{xo}^{*} = (R + L\frac{d}{dt}) i_{xo}$. The R and L are resistance and inductance of an arm inductor, and all arm inductors in the MMC are assumed as identical.

$$\begin{aligned} &-V_{dc} + v_{xuL} + v_{xlL} + v_{xP} + v_{xN} = 0 \\ &\Leftrightarrow -V_{dc} + 2 \cdot \left(R + L\frac{d}{dt} \right) \left(\frac{i_{xu} + i_{xl}}{2} \right) + v_{xP} + v_{xN} = 0. \end{aligned} \tag{7}$$

$$v_{xo}^{*} = \frac{V_{dc}}{2} - \frac{v_{xP} + v_{xN}}{2} . \tag{8}$$

$$v_{xP}^{*}\big|_{cir} = \frac{V_{dc}}{2} - v_{xo}^{*}, \quad v_{xN}^{*}\big|_{cir} = \frac{V_{dc}}{2} - v_{xo}^{*} . \tag{9}$$

So, the upper and lower arm voltage references to regulate inner circulating currents can be derived as (9).

Next, a sum of (5) and (6) can be presented as (10), where v_{xn}^{*} is the pole voltage reference of the corresponding phase.

$$\begin{aligned} &v_{xuL} - v_{xlL} + v_{xP} - v_{xN} + 2v_{xn}^{*} = 0 \\ &\Leftrightarrow (R + L\frac{d}{dt})(i_{xu} - i_{xl}) + v_{xP} - v_{xN} + 2v_{xn}^{*} = 0. \end{aligned} \tag{10}$$

The pole voltage reference including the arm inductor voltage, which is incurred by the phase current, is defined as v_{xn}^{**} like (11). Thus, the arm voltage reference to control the output phase current can be determined by (12).

$$v_{xn}^{**} = v_{xn}^{*} + \frac{1}{2}(R + L\frac{d}{dt}) i_{xs} . \tag{11}$$

$$v_{xn}^{**} = -\frac{v_{xP} - v_{xN}}{2} \quad \Leftrightarrow \quad v_{xP}^{*}\big|_{out} = -v_{xn}^{**}, \quad v_{xN}^{*}\big|_{out} = v_{xn}^{**} . \tag{12}$$

Overall arm voltage reference can be denoted as (13) from the superposition of (9) and (12), because these two kinds of arm voltage references in (9) and (12) are decoupled independently.

$$\begin{aligned} v_{xP}^{*} &= v_{xP}^{*}\big|_{cir} + v_{xP}^{*}\big|_{out} = \frac{V_{dc}}{2} - v_{xn}^{**} - v_{xo}^{*} , \\ v_{xN}^{*} &= v_{xN}^{*}\big|_{cir} + v_{xN}^{*}\big|_{out} = \frac{V_{dc}}{2} + v_{xn}^{**} - v_{xo}^{*} . \end{aligned} \tag{13}$$

B. The Energy in the Arm Capacitor

Total power of each arm is represented as (14)-(15), and the sum and difference of them are calculated by (16)-(17). In addition, $v_{xn}^{**} = v_{xs}^{**} + v_{sn}$ holds as shown in Fig. 1 through voltage difference between node 's' and node 'n'. And, this voltage difference is a common mode voltage, v_{sn} .

$$\begin{aligned} P_{xP} &= v_{xP}^{*} \cdot i_{xu} = \left(\frac{V_{dc}}{2} - v_{xn}^{**} - v_{xo}^{*} \right) \left(i_{xo} + \frac{i_{xs}}{2} \right) \\ &= \frac{V_{dc}}{2} i_{xo} - \frac{1}{2} v_{xn}^{**} i_{xs} - v_{xo}^{*} i_{xo} + \frac{V_{dc}}{4} i_{xs} - v_{xn}^{**} i_{xo} - \frac{1}{2} v_{xo}^{*} i_{xs} . \end{aligned} \tag{14}$$

$$\begin{aligned} P_{xN} &= v_{xN}^{*} \cdot i_{xl} = \left(\frac{V_{dc}}{2} + v_{xn}^{**} - v_{xo}^{*} \right) \left(i_{xo} - \frac{i_{xs}}{2} \right) \\ &= \frac{V_{dc}}{2} i_{xo} - \frac{1}{2} v_{xn}^{**} i_{xs} - v_{xo}^{*} i_{xo} - \frac{V_{dc}}{4} i_{xs} + v_{xn}^{**} i_{xo} + \frac{1}{2} v_{xo}^{*} i_{xs} . \end{aligned} \tag{15}$$

$$P_{xP} + P_{xN} = V_{dc} i_{xo} - v_{xs}^{**} i_{xs} - v_{sn} i_{xs} - 2v_{xo}^{*} i_{xo} . \tag{16}$$

$$P_{xP} - P_{xN} = 0.5 V_{dc} i_{xs} - 2v_{xs}^{**} i_{xo} - 2v_{sn} i_{xo} - v_{xo}^{*} i_{xs} . \tag{17}$$

The sum of power of both upper and lower arm derived as (16), is defined as a leg power which means difference between input power from DC-link and AC output power. The second term of the right-hand side in (16), $v_{xs}^{**} i_{xs}$ is multiplication of two fundamental frequency components, and the term has DC and 2nd order harmonic components. In the case that the leg power has DC component in steady-state, the capacitor voltages in the leg can diverge and the system cannot maintain the stable state. Hence, DC power of (16) should be eliminated by controlling the circulating current with DC components. Furthermore, the 2nd order harmonic component can also be eliminated by the circulating current simultaneously to suppress the severe fluctuation of cell capacitor voltage. This control strategy is called as an averaging control.

The capacitor power difference between the upper and lower arm, derived as (17), affects balance of cell capacitor voltage of arms. The first term of the right-hand side in (17), $0.5 V_{dc} i_{xs}$, has fundamental frequency component. Thus, if the output phase current has DC or low frequency component, the voltage difference between arms can diverge. In order to operate MMC at DC and low frequency, the power difference should be compensated using i_{xo} . However, i_{xo} is already used for eliminating $v_{xs}^{**} i_{xs}$ in (16). To balance the power difference between arms, a control strategy exploiting common mode voltage (v_{sn}) has been devised in this paper. The common mode voltage, v_{sn} , can be regarded as an additional degree of freedom for controllability because the common mode voltage

does not affect to the output phase current. It is the natural to select the frequency of the common mode voltage as a high frequency to minimize the fluctuation of the cell capacitor voltage due to the common mode voltage itself. Hence, the third term of the right-hand side in (17), $2v_{sn}i_{xo}$ can be used for the balance of power of arms with high frequency component in v_{sn} and i_{xo}. This control strategy is called as a balancing control. And, the low and high frequency elements can be segregated from v_{sn} and i_{xo} as (18) and (19), where "~" and "^" mean low and high frequency component respectively.

$$i_{xo} = \tilde{i}_{xo} + \hat{i}_{xo} . \tag{18}$$

$$v_{sn} = \hat{v}_{sn} . \tag{19}$$

C. Averaging Control

1) Low Frequency Mode:

Eq. (16) can be written as (20) substituting (18)-(19). The voltage v_{xo}^{*} might be omitted in (16) under the assumption that the impedance of the arm inductor is small enough to neglect the voltage drop.

$$\begin{aligned} &P_{xP} + P_{xN} \approx V_{dc}i_{xo} - v_{xn}^{**}i_{xs} \\ &= V_{dc}i_{xo} - (v_{xs}^{**} + v_{sn})i_{xs} = V_{dc}\tilde{i}_{xo} + V_{dc}\hat{i}_{xo} - v_{xs}^{**}i_{xs} - \hat{v}_{sn}i_{xs} . \end{aligned} \tag{20}$$

The pulsation of the energy is far more affected by the low frequency component than by the high frequency component. The low frequency power component in (20) can be controlled as null denoted in (21).

$$P_{xP} + P_{xN}\big|_{low\ freq.} = V_{dc}\tilde{i}_{xo} - v_{xs}^{**}i_{xs} = 0 . \tag{21}$$

$$\tilde{i}_{xo} = \frac{v_{xs}^{**}i_{xs}}{V_{dc}} . \tag{22}$$

Eq. (21) can be met by (22) which has DC and 2nd order harmonic frequency components. The averaging control strategy is depicted as a control block diagram in Fig. 2(a). E_{leg} is the energy of the leg, and it can be represented as (23). E_{leg}^{*} is the reference energy of the leg, and it is set as (24), where v_c^{*} is V_{dc}/N.

$$\begin{aligned} E_{leg} &= \frac{1}{2}C_{cell}\sum_{i=1}^{2N}v_{ci}^2 = \frac{1}{2}\cdot 2N\frac{C_{cell}}{2N}\sum_{i=1}^{2N}v_{ci}^2 \\ &= NC_{cell}\frac{1}{2N}\sum_{i=1}^{2N}v_{ci}^2 = NC_{cell}\left\langle v_c^2\right\rangle_{avg} . \end{aligned} \tag{23}$$

$$E_{leg}^{*} = \frac{1}{2}\frac{C_{cell}}{2N}4N^2v_c^{*2} = NC_{cell}v_c^{*2} . \tag{24}$$

The feed-forwarding term, P_{leg}^{ff}, in Fig. 2(a) is derived as (25) by the aforementioned equation (22).

$$P_{leg}^{ff} = v_{xs}^{*}i_{xs} . \tag{25}$$

2) Normal Frequency Mode:

In normal frequency mode, the frequency of the 2nd order harmonic is high enough and the voltage fluctuation of the cell capacitor due to the harmonic is tolerable. So, in the normal frequency mode the circulating current is controlled to have only DC component to minimize the conduction loss caused by the circulating current. And the current of each leg is DC and its magnitude is $I_{dc}/3$, where I_{dc} is DC component of i_{dc} in Fig. 1(a).

D. Balancing Control

1) Low Frequency Mode:

The difference in power between upper and lower arm can also be rearranged as (26) from (17)-(19).

$$\begin{aligned} &P_{xP} - P_{xN} \approx \frac{1}{2}V_{dc}i_{xs} - 2v_{xn}^{**}i_{xo} = \frac{1}{2}V_{dc}i_{xs} - 2(v_{xs}^{**} + v_{sn})i_{xo} \\ &= \frac{1}{2}V_{dc}i_{xs} - 2v_{xs}^{**}\tilde{i}_{xo} - 2v_{xs}^{**}\hat{i}_{xo} - 2\hat{v}_{sn}\tilde{i}_{xo} - 2\hat{v}_{sn}\hat{i}_{xo} . \end{aligned} \tag{26}$$

Low frequency power component in (26) can be extracted and $\tilde{i}_{xo}$ can be substituted with (22). And, the low frequency component can be controlled to null denoted as (27).

$$\begin{aligned} &P_{xP} - P_{xN}\big|_{low\ freq.} = \frac{1}{2}V_{dc}i_{xs} - 2v_{xs}^{**}\tilde{i}_{xo} - 2\hat{v}_{sn}\hat{i}_{xo}\Big|_{low\ freq.} \\ &= \frac{1}{2}V_{dc}i_{xs} - 2v_{xs}^{**}\frac{v_{xs}^{**}i_{xs}}{V_{dc}} - 2\hat{v}_{sn}\hat{i}_{xo}\Big|_{low\ freq.} = 0. \end{aligned} \tag{27}$$

Nullifying the low frequency component by (27) can be done by the low frequency component of $\hat{v}_{sn}\hat{i}_{xo}$. $\hat{v}_{sn}$ and $\hat{i}_{xo}$ can be defined by (28)-(29), and ω_h stands for the angular speed of high frequency component, V_{sn} for the magnitude of common mode voltage, and $\tilde{I}_{xo}$ for the magnitude of high frequency circulating current which may have several low frequency components.

$$\hat{v}_{sn} = V_{sn}\cos(\omega_h t) . \tag{28}$$

$$\hat{i}_{xo} = \tilde{I}_{xo}\cos(\omega_h t) . \tag{29}$$

The low frequency component of the power associated with the common mode voltage and the circulating current can be derived as (30).

$$\begin{aligned} &2\hat{v}_{sn}\hat{i}_{xo}\Big|_{low\ freq.} = 2V_{sn}\tilde{I}_{xo}\cos^2(\omega_h)\Big|_{low\ freq.} \\ &= V_{sn}\tilde{I}_{xo} = \frac{1}{2}V_{dc}i_{xs} - 2v_{xs}^{**}\frac{v_{xs}^{**}i_{xs}}{V_{dc}} \\ &\Leftrightarrow \tilde{I}_{xo} = \frac{1}{V_{sn}}\left(\frac{1}{2}V_{dc}i_{xs} - 2\frac{(v_{xs}^{**})^2i_{xs}}{V_{dc}}\right). \end{aligned} \tag{30}$$

The balancing control strategy is depicted as a block diagram in Fig. 2(b). The difference in energy between upper and lower arm (E_{err}) is derived as (31). E_{err}^{*} is the reference of energy difference, and should be set to zero to prevent diverge of the voltage at each arm. And P_{err}^{ff}, which stands for the feed-forwarding term in Fig. 2(b), can be deduced as (32) by (30).

$$E_{err} = E_{upper} - E_{lower} = \frac{1}{2}NC_{cell}\left\{\left\langle v_{cu}^2\right\rangle_{avg} - \left\langle v_{cl}^2\right\rangle_{avg}\right\} . \tag{31}$$

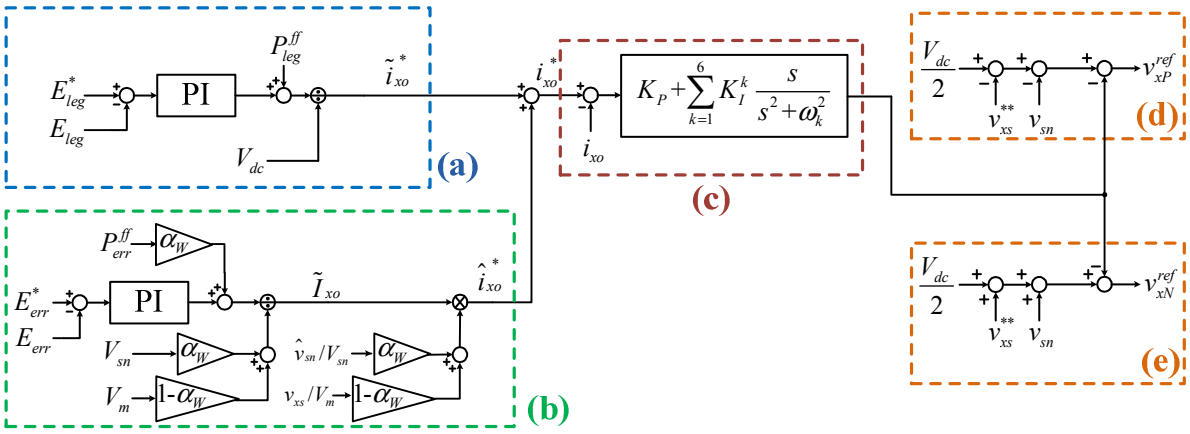

Figure 2. Proposed control scheme for variable-speed drive: (a) averaging controller, (b) balancing controller, (c) circulating current controller, (d) upper arm voltage reference, and (e) lower arm voltage reference. α_W is weighting factor for switchover, which is described in section *F*.

$$P_{err}^{ff} = \frac{1}{2} V_{dc} i_{xs} - 2\frac{(v_{xs}^{**})^2 i_{xs}}{V_{dc}}. \tag{32}$$

2) Normal Frequency Mode:

As the operation frequency increases, the margin of the common mode voltage decreases. So, the common mode voltage becomes little effective component for balancing control. P_{err}^{ff} also cannot contribute to balancing, because it is derived from v_{sn}. As operating frequency increases, however, the fluctuation of cell capacitor voltage is within permissible range. In normal frequency mode, therefore, it is sufficient only to eliminate inevitable DC unbalance. The balancing can be achieved by using $v_{xs}^{**}\hat{i}_{xo}$ in (26). And, by regulating $\hat{i}_{xo}$ to have fundamental frequency component, DC unbalance can be suppressed.

E. Circulating Current Control

1) Low Frequency Mode:

The circulating current reference produced from the averaging controller has DC and low frequency components. In addition, the output of the balancing controller has high frequency component. Thus, it is essential to control each frequency component correspondingly. It can be assumed that phase voltage reference and phase current are defined by $v_{xs}^{**} = V_m \cos(\omega_s t)$ and $i_{xs} = \mathrm{I}_m \cos(\omega_s t + \phi)$ respectively, with the magnitude of the phase voltage V_m and of the phase current I_m, the load angle ϕ between voltage and current, and $\omega_s = 2\pi f_s$, f_s being the output frequency. The low frequency circulating current satisfying (21) can be deduced as (33). It has DC and 2nd order harmonic component ($2\omega_s$). Meanwhile, the high frequency circulating current satisfying (27) can be deduced as (34). The current has four kinds of frequency component specified in (34), and the components are, $\omega_h - 3\omega_s$, $\omega_h - \omega_s$, $\omega_h + \omega_s$, and $\omega_h + 3\omega_s$.

$$\begin{aligned}\tilde{i}_{xo} &= \frac{v_{xs}^{**} i_{xs}}{V_{dc}} = \frac{V_m I_m}{V_{dc}} \cos(\omega_s t)\cos(\omega_s t + \phi) \\ &= \frac{V_m I_m}{2V_{dc}} \left(\cos\phi + \cos(2\omega_s t + \phi)\right).\end{aligned} \tag{33}$$

$$\begin{aligned}\hat{i}_{xo} &= \tilde{I}_{xo}\cos(\omega_h t) = \frac{1}{V_{sn}}\left(\frac{1}{2}V_{dc} i_{xs} - 2\frac{(v_{xs}^{**})^2 i_{xs}}{V_{dc}}\right)\cos(\omega_h t) \\ &= \left(\frac{V_{dc} I_m}{4V_{sn}} - \frac{8V_m^2 I_m}{V_{dc}}\right)\begin{Bmatrix}\cos((\omega_h - \omega_s)t - \phi) \\ +\cos((\omega_h + \omega_s)t + \phi)\end{Bmatrix} \\ &\quad - \frac{4V_m^2 I_m}{V_{dc}}\begin{Bmatrix}\cos((\omega_h - \omega_s)t + \phi) + \cos((\omega_h + \omega_s)t - \phi) \\ +\cos((\omega_h - 3\omega_s)t - \phi)\cos((\omega_h + 3\omega_s)t + \phi)\end{Bmatrix}.\end{aligned} \tag{34}$$

Under the consideration of (33) and (34), six kinds of frequency component of the circulating current should be regulated. This paper introduces Proportional and Resonant (PR) regulator which has the narrow band and infinite gain at the displacement of the resonant pole [10]. As shown as Fig. 2(c), circulating current controller consists of one proportional controller and six resonant controllers. Consequently, voltage reference to regulate the circulating current, (v_{xo}^{*}), can be made up of the superposition of outputs of PR regulator, that is depicted in Fig. 2(c).

2) Normal Frequency Mode:

As mentioned at normal frequency mode of averaging and balancing control, the circulating current should be regulated to have only DC component. So, in normal frequency mode, all references to R-controllers except DC controller ($k = 1$, $\omega_1 = 0$ in Fig. 2(c)) have to be set as null.

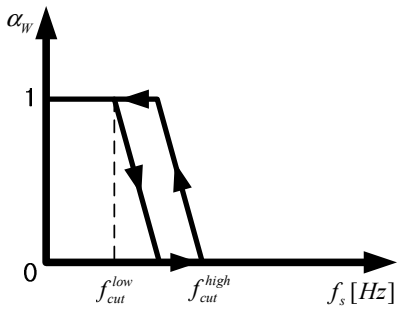

Figure 3. The relationship between operating frequency and weighting factor.

F. Switchover Method between Two Modes

As mentioned before, because the 2nd order harmonic and high frequency component of the circulating current is only injected in low operating frequency operation, the circulating current reference is changed depending on operating frequency. A switchover strategy between low and high frequency modes shown in Fig. 3 is devised by weighting factor (α_w). And, this factor is applied to switchover of balancing control as well as circulating current control as shown in Fig. 2. In addition, the strategy has the hysteresis band to prevent ringing during the switchover.

III. Experimental Results

The proposed control scheme was validated by a prototype 10kVA MMC. The parameter of system is summarized at Table 1. As the number of cells in each arm, N, equals 2, total 12 cells are used for three-phase system. Each cell capacitor voltage is controlled as 155V. And the level-shifted Phase Opposite Disposition PWM (POD-PWM) is applied to each arm voltage reference [11]-[12]. The MMC was connected to drive 11kW 8-pole Permanent Magnet Synchronous Machine (PMSM) which is coupled to an Induction Machine (IM) for applying load torque to PMSM. The specification of PMSM is summarized at Table 2. The experiments were carried out in three cases which are the low frequency operation, the normal frequency operation, and the operation from starting to normal frequency mode.

TABLE I. Circuit Parameters and Experiment Conditions

Rated power	S_{MMC}	10kVA
DC-link voltage source	V_{dc}	310V
Arm inductor	L	2mH
Cell capacitor	C_{cell}	4400μF
Carrier frequency	f_{sw}	5kHz

TABLE II. Specification of the PMSM

Rated active power	P_{PMSM}	11kW
Rated line-to-line rms voltage	V	200V
Rated rms line current	I	58.6A
Rated rotational speed	ω_{rm}	1750r/min
Pole pair number	pp	4

A. The Low Frequency Operation

Fig. 4 shows the low frequency operation at 1Hz ($\omega_{rm} = 15\,r/\min$) with load torque 40% ($T_L = 24N \cdot m$). The *u*-phase current (i_{us}) is sinusoidal with fundamental frequency, 1Hz. The cell capacitor voltages are also well regulated within around 15V regardless of this extremely low frequency operation. The fluctuation of the cell voltages is around 10% of the nominal DC link voltage of cell. The *u*-phase circulating current (i_{uo}) has six frequency components. Especially, it reveals the dominant frequencies, namely, 2nd order harmonic and injected high frequency, 180Hz.

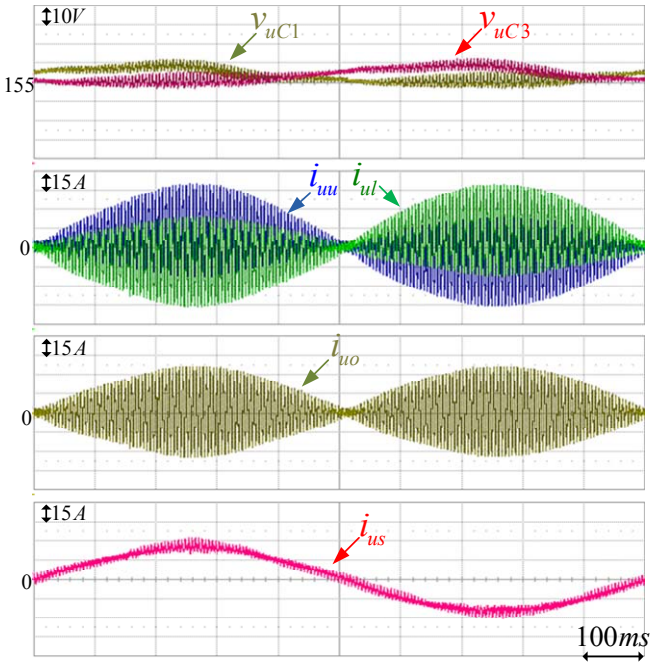

Figure 4. Experimental waveforms when rotating speed is 15 r/min and load torque is 40%.

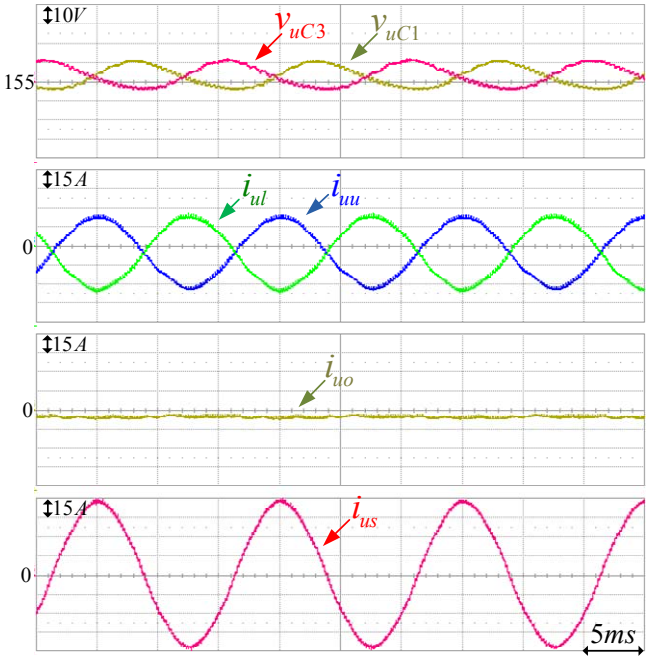

Figure 5. Experimental waveforms when rotating speed is 1000 r/min and load torque is 100%.

B. The Normal Frequency Operation

In Fig. 5, the machine operates 1000 r/min with load torque 100% ($T_L = 60N \cdot m$) in the normal frequency mode. The

pulsation of cell capacitor voltages is around 12V (8%), and i_{uo} in normal frequency mode has almost DC component as designed. As mentioned above, regulating inner circulating current as DC helps reduction of the conduction loss.

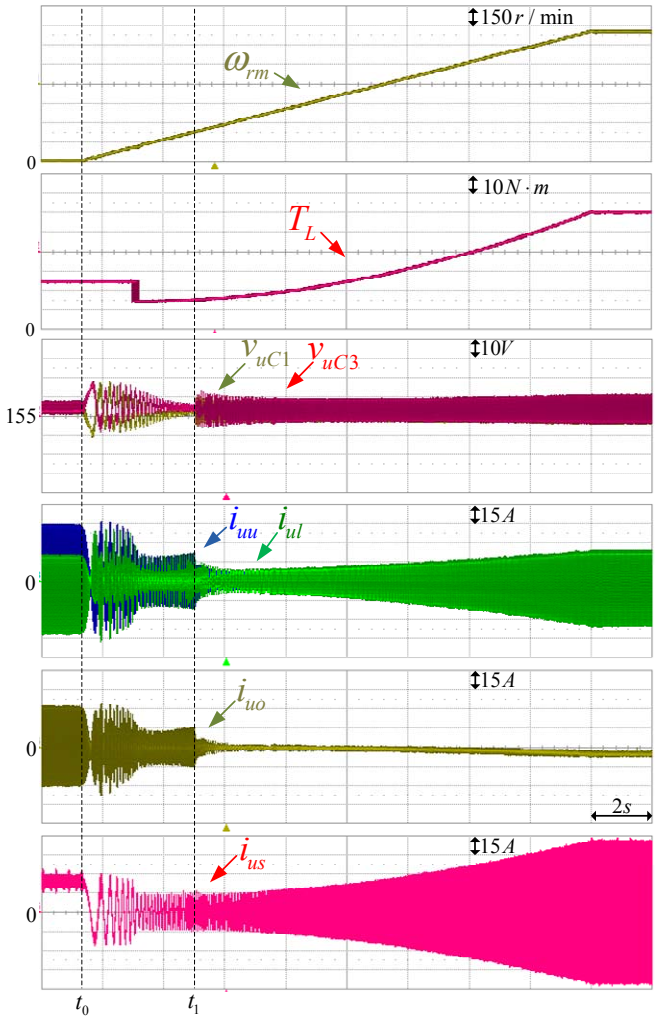

Figure 6. Experimental waveforms in the conditions of variable speed drive from starting to 1000 r/min with starting torque(40%) and the increasing load torque depending on rotating speed.

C. *The Operation from Starup to Normal Mode*

Fig. 6 shows the operation from standstill ($t = t_0$) to normal frequency mode, 1000 r/min. In order to conduct the switchover operation in practical application of variable speed drive such as fans, blowers, or pumps, the load torque was applied in proportional to the square of the speed. Also, the startup torque is included in the torque profile. As the startup torque is applied as 40%, the phase current before $t = t_0$ is regulated DC. At $t = t_1$, the switchover process starts, and the operating mode changes to the normal frequency operation mode. As shown in Fig. 6, it has been confirmed that all control strategies depicted in Fig. 2 were well implemented and incorporated properly to drive variable speed AC machine in overall speed including standstill by MMC.

IV. CONCLUSIONS

In this paper, several control strategies for variable-speed AC drive by the MMC have been presented. To overcome the difficulties of the power balance between cells and arms of MMC over wide operating speeds, the operation mode is divided into two, low frequency operation mode and normal frequency operation mode. For smooth switchover between two modes, a weighting factor depending on the operating speed with hysteresis band has been introduced. The averaging control, balancing control, and circulating current control are devised at each operating mode. The variable speed motor drive with the control schemes has been verified by experiments using 10kVA prototype MMC system. The fluctuation of the cell voltage has been suppressed within 10% of nominal DC link voltage of the cell.

ACKNOWLEDGMENT

The authors would like to thank Hyundai Heavy Industries and LSIS Co., Ltd for their friendly support.

REFERENCES

[1] M. Winkelnkemper, A. Korn, and P. Steimer, “A modular direct converter for transformerless rail interties,” in Proc. IEEE International Symposium on Industrial Electronics 2010, pp. 562-567.

[2] A. Lesnicar, R. Marquardt, “An innovative modular multilevel converter topology suitable for a wide power range,” Power Tech Conference Proceedings, 2003 IEEE Bologna, vol. 3, June 23-26, 2003.

[3] A. Lesnicar, and R. Marqardt, “A new modular voltage source inverter topology,” in Proc, 10th European Power Electronics Conference, 2003, pp. 1-10.

[4] B. Gemmell, J. Dorn, D. Retzmann, and D. Soerangr, “Prospects of multilevel VSC technologies for power transmission,” in Proc. The HVDC Transmission Workshop, Rome, Italy, Nov.2008, pp. 1-16

[5] G. Bergna, E. Berne, P. Egrot, P. Lefranc, A. Arzande, J. Vannier, and M. Molinas, “An Energy-based Controller for HVDC Modular Multilevel Converter in Decoupled Double Synchronous Reference Frame for Voltage Oscillations Reduction,” Industrial Electronics, IEEE Transactions on , vol.PP, no.99, pp.1, 0.

[6] M. Hagiwara, K. Nishimura, and H. Akagi, “A Medium-Voltage Motor Drive With a Modular Multilevel PWM Inverter,” IEEE Trans. Power Electron., vol. 25, no. 7, pp. 1786-1799, Jul. 2010.

[7] J. Kolb, F. Kammerer, and M. Braun, “Straight forward vector control of the Modular Multilevel Converter for feeding three-phase machines over their complete frequency range,” IECON 2011 – 37th Annual Conference of IEEE Industrial Electronics Society, pp. 1596-1601, Nov. 2011.

[8] A. J. Korn, M. Winkelnkemper, and P. Steimer, “Low Output Frequency Operation of the Modular Multi-Level Converter,” in Preceedings of the IEEE Energy Conversion Congress and Exposition 2010, pp. 3993-3997, Sept. 2010.

[9] A. Antonopoulos, K. Ilves, L. Angquist, and H. -P. Nee, “On interaction between internal converter dynamics and current control of high-performance high-power AC motor drives with modular multilevel converters,” in Conf. Rec. IEEE-ECCE 2010, pp. 4293-4298.

[10] D. N. Zmood and D. G. Holmes, “Stationary frame current regulation of PWM inverters with zero steady-state error,” IEEE Trans. Power Electron., vol. 18, no. 3, pp. 814-822, May. 2003.

[11] S. Rohner, S. Bernet, M. Hiller, and R. Sommer, “Modulation, Losses, and Semiconductor Requirements of Modular Multilevel Converters,” IEEE Trans. Industrial Electronics, vol. 57, no. 8, August 2010.

[12] Tengfei, W. and Z. Yongqiang. "Analysis and comparison of multicarrier PWM schemes applied in H-bridge cascaded multi-level inverters." in Industrial Electronics and Applications (ICIEA), 2010 the 5th IEEE Conference on.